

# Pomerons

P V Landshoff

*DAMTP, University of Cambridge*

---

## Abstract

New small- $x$  data indicate the existence of two pomerons: the usual soft pomeron with intercept close to 1.08, and a hard pomeron with intercept about 1.4

---

## 1 The soft pomeron

The existence of the soft pomeron is now well-established, even if the precise value of its intercept  $1 + \epsilon_1$  is not agreed. Donnachie and I believe[1] that  $\epsilon_1$  is close to 0.08, while others[2–4] believe it is close to 0.1. It seems that, to a good approximation, the trajectory is linear:

$$\alpha_1(t) = 1 + \epsilon_1 + \alpha'_1 t \quad (1)$$

The value of the slope has been known for over a quarter of a century[5] to be

$$\alpha'_1 = 0.25 \text{ GeV}^{-2} \quad (2)$$

This value has since been confirmed by comparison between elastic-scattering data from the ISR and the Tevatron: see figure 1. The value (2) correctly predicted the observed shrinkage of the forward peak.

Another verification comes from the change in the differential cross section for the process  $\gamma p \rightarrow \rho p$  with increasing energy. It is essential to include not just soft-pomeron exchange, but also  $f_2, a_2$  exchange, for which the trajectory is

$$\alpha_R(t) = 1 + \epsilon_R + \alpha'_R t \quad (3)$$

with

$$\epsilon_R \approx -0.5 \quad \alpha'_R \approx 0.9 \text{ GeV}^{-2} \quad (4)$$

---

*Email address:* pvl@damtp.cam.ac.uk (P V Landshoff).

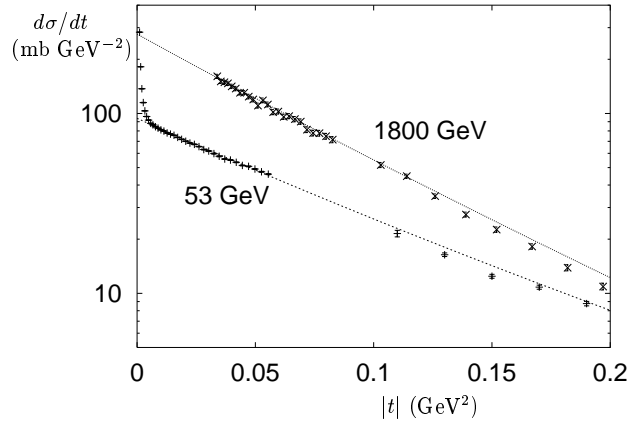


Fig. 1.  $pp$  elastic scattering[6] at  $\sqrt{s} = 53$  GeV and[7]  $\bar{p}p$  at  $\sqrt{s} = 1800$  GeV. The curves verify the value of the soft-pomeron slope to be  $\alpha'_1 = 0.25 \text{ GeV}^{-2}$ .

A fit to the low-energy data is shown in figure 2. The same fit continues to perform well when extrapolated to high energy: figure 3.

## 2 Two pomerons

While the soft pomeron accounts well for the rise with energy of cross sections for soft processes, data for hard and semi-hard processes reveal an additional contribution. The data are described very well[10,11] by the assumption that this contribution is a second pomeron. If its trajectory is linear:

$$\alpha_0(t) = 1 + \epsilon_0 + \alpha'_0 t \quad (5)$$

then we find that experiment requires

$$\epsilon_0 \approx 0.4 \quad \alpha'_0 \approx 0.1 \text{ Gev}^{-2} \quad (6)$$

Consider first the proton structure function  $F_2(x, Q^2)$ . The pomeron exchanges contribute at small  $x$

$$F_2(x, Q^2) \sim \sum_{i=0,1} f_i(Q^2) x^{-\epsilon_i} \quad (7)$$

Figure 4 shows the coefficient functions  $f_i(Q^2)$  extracted from the data[12–14] for  $x < 0.02$  at each available value of  $Q^2$ , for two choices of  $\epsilon_0$ . We see that if we suppose that the soft-pomeron coefficient function  $f_1(Q^2)$  becomes constant at large  $Q^2$  a larger value of  $\epsilon_0$  is favoured than if we suppose that it decreases with increasing  $Q^2$ . We find[11] that either hypothesis gives a good fit to the data. In either case, the hard-pomeron coefficient function increases

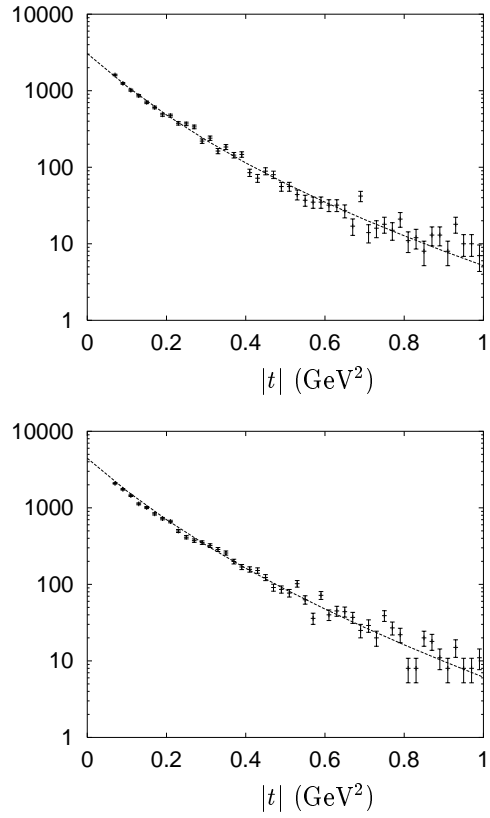


Fig. 2. Data[8] for  $\gamma p \rightarrow \rho p$  at  $\sqrt{s} = 6.86 \text{ GeV}$  (upper figure) and  $10.8 \text{ GeV}$  (lower figure) with Regge curves. The data are events per  $0.02 \text{ GeV}^{-2}$ .

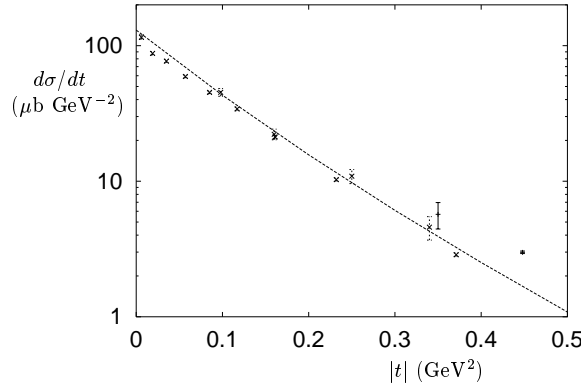


Fig. 3. ZEUS data[9] for  $\gamma p \rightarrow \rho p$  with the Regge-model prediction. The lower- $t$  data are at  $\sqrt{s} = 71.7 \text{ GeV}$  and the higher- $t$  data at  $94 \text{ GeV}$ .

at large  $Q^2$ ; the best fit we have found corresponds to a power behaviour

$$f_1(Q^2) \sim Q^{\epsilon_0} \quad (8)$$

at large  $Q^2$ .

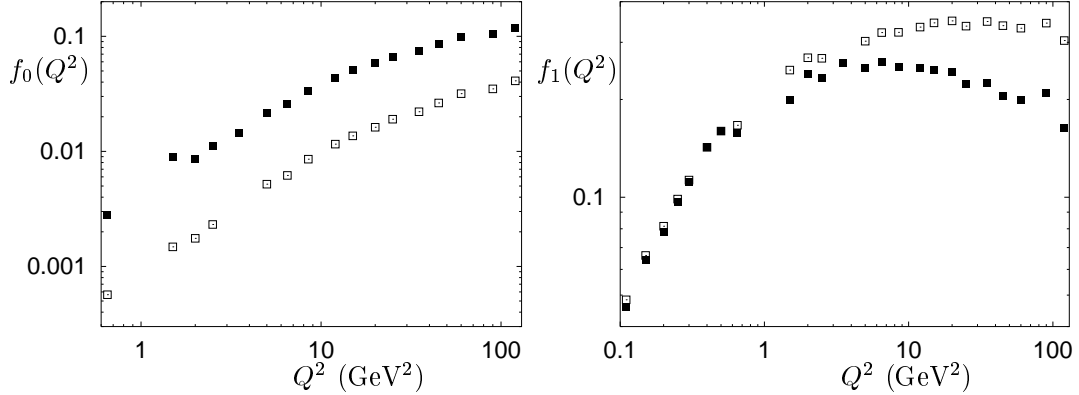


Fig. 4. Fits to the coefficient functions  $f_0(Q^2)$  and  $f_1(Q^2)$  of (7) extracted from H1 and ZEUS data[12–14]. The black points are for  $\epsilon_0 = 0.36$  and the white points are for  $\epsilon_0 = 0.5$ .

The data are now so very accurate that, even at very small  $x$ , the simple-power fit (7) needs modifying, to take account of the fact that  $F_2(x, Q^2) \rightarrow 0$  as  $x \rightarrow 1$ . The simplest assumption, consistent with the dimensional-counting rules, is to multiply each term by  $(1-x)^7$ . This is surely over-simple, but should be better than not including any such factor. We fit to data for  $x < 0.001$  and then these factors have a small effect, but it is not completely negligible. The fit is shown in figure 5 and has essentially just 4 free parameters, including  $\epsilon_0$ . Although we used only data for  $x < 0.001$  to make the fit, we see that it is quite good up to larger  $x$ , and all the way from  $Q^2 = 0.045$  to  $5000$  GeV $^2$ .

Somewhat remarkably, the data[15] for the charm component  $F_2^c(x, Q^2)$  of  $F_2(x, Q^2)$  have the striking property that over a wide range of  $Q^2$  they behave as a fixed power of  $x$ . They are described very well by a hard-pomeron term alone. Further, the hard pomeron seems to be flavour-blind. Figure 6 shows ZEUS data together with  $\frac{2}{5}$  the hard-pomeron contribution to  $F_2(x, Q^2)$ . The factor  $\frac{2}{5}$  is just  $e_c^2/(e_u^2 + e_d^2 + e_s^2 + e_c^2)$ . There are considerable uncertainties about these data, because they are obtained using a very large extrapolation in  $p_T$ , but on the face of it they are very compelling evidence for the hard-pomeron concept.

### 3 Real photons

The total cross section for real-photon absorption is

$$\sigma^{\gamma p} = \frac{4\pi^2\alpha}{Q^2} F_2^c(x, Q^2) \Big|_{Q^2=0} \quad (9)$$

Figure 7 shows that hard-pomeron exchange continues to describe charm-production data down to  $Q^2 = 0$ .

A key question is whether all of the hard-pomeron component of  $F_2(x, Q^2)$ , not just the  $c$ -quark part, survives at  $Q^2 = 0$ . That is, does the hard-pomeron part

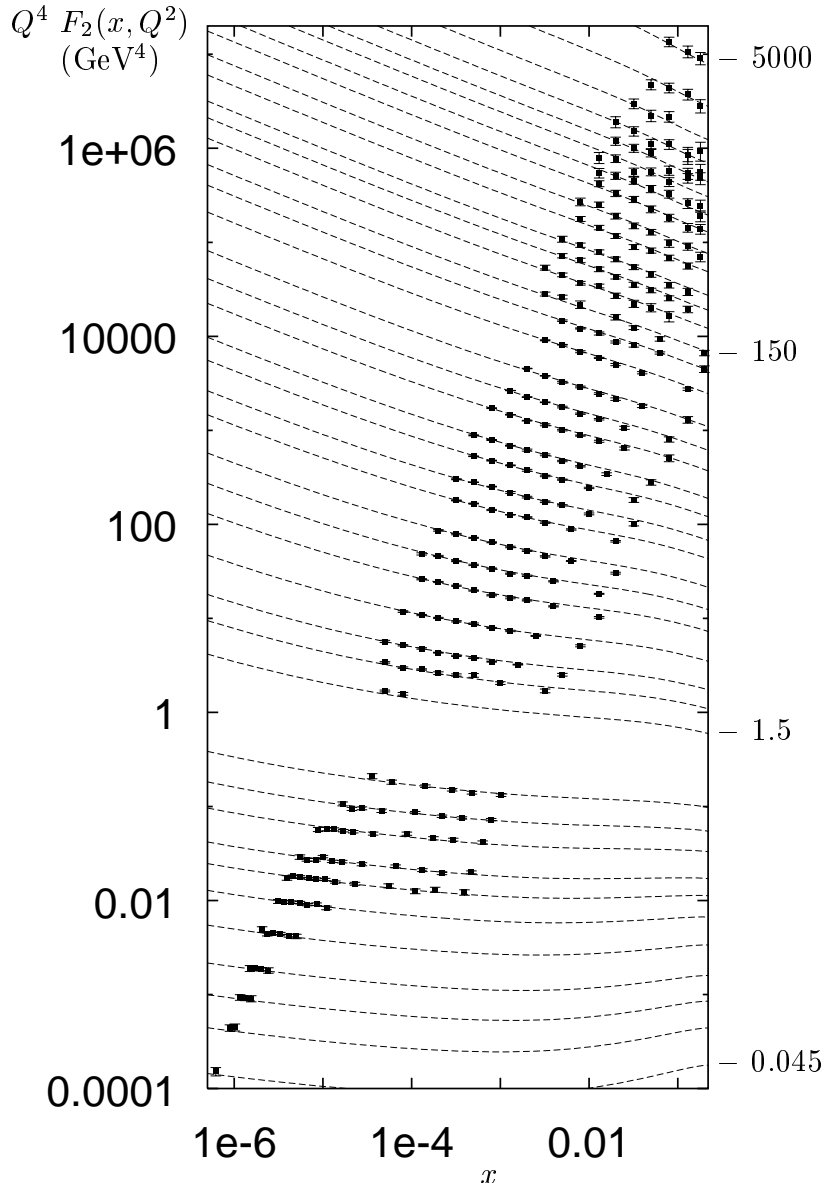


Fig. 5. Regge fit to data for  $F_2(x, Q^2)$  for  $Q^2$  between 0.045 and 5000  $\text{GeV}^2$ . The parameters were fixed using only data for  $x < 0.001$ .

of  $F_2(x, Q^2)$  exist already at  $Q^2 = 0$ , or is it rather generated by perturbative evolution as  $Q^2$  increases? The latter view is the conventional one; I believe that it is wrong, but the data do not yet allow us to decide one way or the other.

Certainly, it is important to include the very accurate data for  $\sigma^{\gamma p}$  in fits to  $F_2(x, Q^2)$ . If one does not, the extrapolation of the fits to  $Q^2 = 0$  misses the data by a mile. That is, the real-photon data provide a significant constraint on fits to  $F_2(x, Q^2)$ . Because these data are at comparatively low energy, they require also an  $(f_2, a_2)$ -exchange term, which we included in our fits[11], but its contribution to the data in figure 5 is extremely small. The data for  $\sigma^{\gamma p}$  are shown in figure 8. The upper curve corresponds to the extrapolation to  $Q^2 = 0$  of the fit shown in figure 5, while the lower curve shows what remains

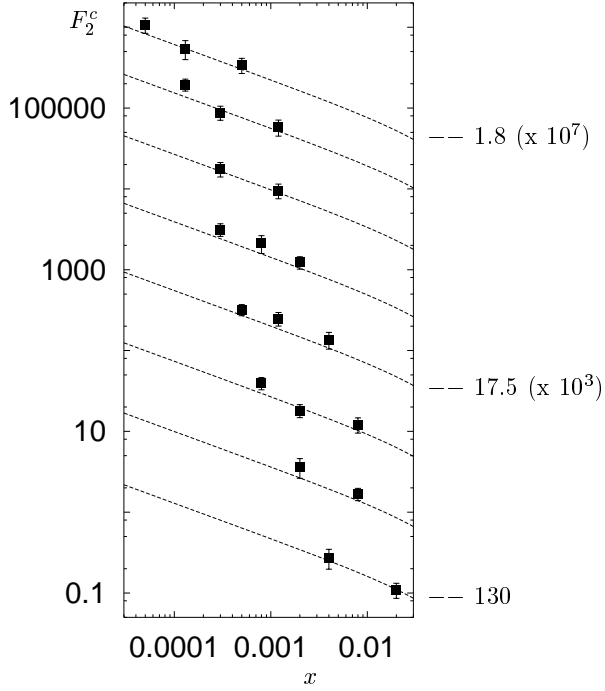


Fig. 6. Data[15] for  $F_2^c(x, Q^2)$  from  $Q^2 = 1.8$  to  $130$   $\text{GeV}^2$ . The curves are the hard-pomeron component of the fit to  $F_2(x, Q^2)$  shown in figure 5, normalised such that the hard pomeron is flavour-blind.

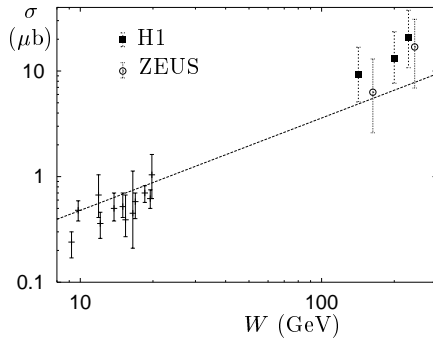


Fig. 7. Extrapolation to  $Q^2 = 0$  of the hard-pomeron contribution to  $F_2^c(x, Q^2)$

when the hard-pomeron component is omitted.

From this figure, we cannot be sure whether a hard-pomeron component is needed at  $Q^2 = 0$ . If the hard pomeron is present in  $\sigma^{\gamma p}$  and  $\sigma^{\gamma\gamma}$ , then presumably it should be there at some level also in  $\sigma^{pp}$ , and it will be interesting to check this at the LHC.

One may ask also whether LEP data[16,17] for  $\sigma^{\gamma\gamma}$  show evidence for a hard-pomeron component at  $Q^2 = 0$ . Unfortunately, the data are highly sensitive to the Monte Carlo used to correct for experimental acceptance. Figure 9 shows this clearly: the two sets of L3 points correspond to different Monte Carols. The curve is obtained by assuming that neither  $\sigma^{\gamma p}$  nor  $\sigma^{pp}$  needs a

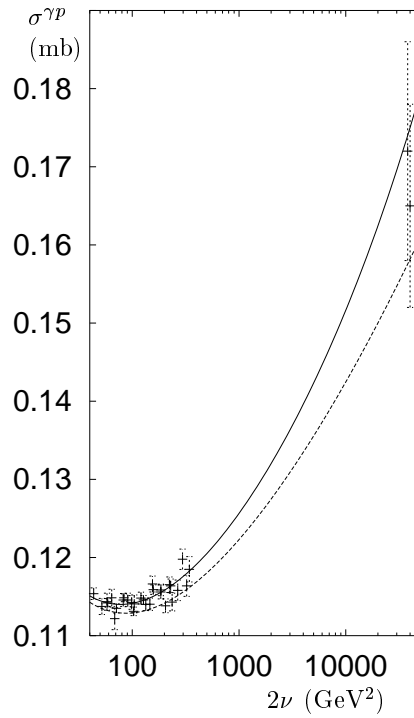


Fig. 8. Data for  $\sigma^{\gamma p}$  with the fit obtained by extrapolating to  $Q^2 = 0$  the fit to  $F_2(x, Q^2)$ . The lower curve has the hard-pomeron component removed.

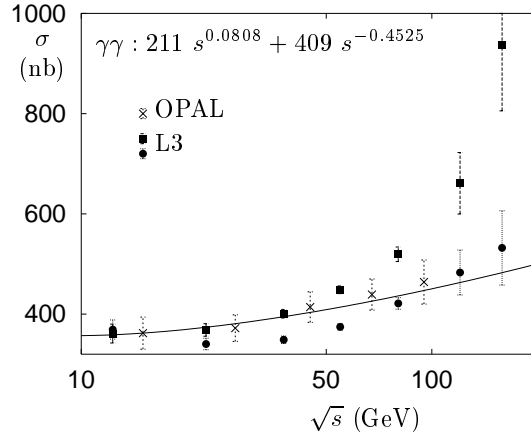


Fig. 9. LEP data[16,17] for  $\sigma^{\gamma\gamma}$ . The curve assumes there is no hard-pomeron contribution.

hard-pomeron term and calculating  $\sigma^{\gamma\gamma}$  by assuming that the soft-pomeron and  $(f_2, a_2)$  components each obey Regge factorisation. At present, no firm conclusion is possible!

## 4 $J/\psi$ photoproduction

I have shown in figure 2 that the rise of the cross section  $\gamma p \rightarrow \rho p$  with energy is consistent with soft-pomeron exchange, and the same is so for  $\gamma p \rightarrow \phi p$ . However, this is not true for  $\gamma p \rightarrow J/\psi p$ , for which the data[18] require a significant hard-pomeron component. The fits in figure 10 correspond to[11]

$$T(s, t) = iF_1(t)G_{J/\psi}(t) \sum_{i=0,1} A_{\mathbb{P}_i} (\alpha'_{\mathbb{P}_i} s)^{\alpha_{\mathbb{P}_i}(t)-1} e^{-\frac{1}{2}i\pi(\alpha_{\mathbb{P}_i}(t)-1)}. \quad (10)$$

Here  $F_1(t)$  is the nucleon Dirac form factor,  $G_{J/\psi}(t)$  is the coupling to the  $\gamma J/\psi$  vertex,  $\alpha_{\mathbb{P}_1}$  is the classical soft-pomeron trajectory and

$$\alpha_{\mathbb{P}_0}(t) = 1.44 + \alpha'_{\mathbb{P}_0} t \quad (11)$$

is the hard-pomeron trajectory. We find it is sufficient to take  $G_{J/\psi}(t)$  constant over the range of  $t$  for which data are available. The differential cross section, figure 10b, shows little or no shrinkage, so the slope of the hard-pomeron trajectory  $\alpha_{\mathbb{P}_0}(t)$  is smaller than  $\alpha'_{\mathbb{P}_1}$ , assuming that it is linear in  $t$ .

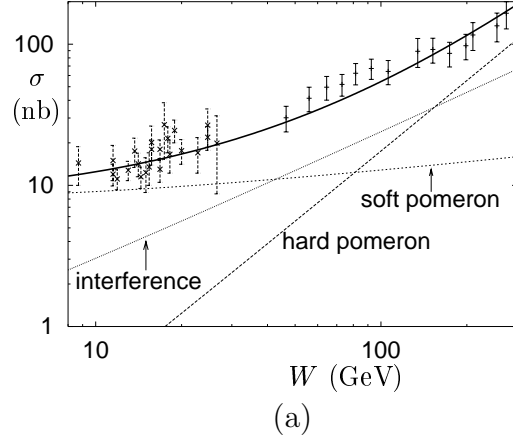
It may be[11] that in  $\gamma p \rightarrow \rho p$ ,  $\phi p$  and  $J/\psi p$  the hard-pomeron contribution is flavour-blind, and then in the first two of these reactions it is swamped by the contribution from soft-pomeron exchange at  $Q^2 = 0$ , but becoming relatively more important as  $Q^2$  increases.

## 5 Perturbative evolution

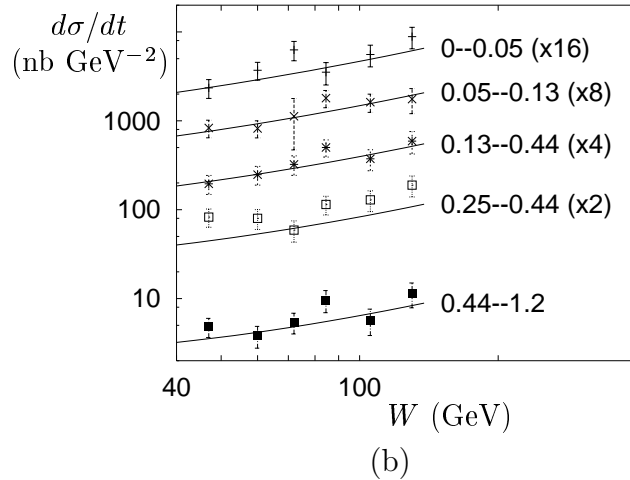
I have to emphasise that Regge theory is not a rival to perturbative evolution: we have to learn how they live together. It is now accepted by most of us that the conventional way to implement perturbative evolution at small  $x$  has unsolved problems. This is because it expands the splitting matrix  $\mathbf{P}(N, \alpha_S)$ , where  $N$  is the Mellin transform variable conjugate to  $x$ , in powers of  $\alpha_S$ , but unfortunately the expansion parameter turns out to be  $\alpha_S/N$ . Therefore the expansion becomes invalid at small  $N$  and some sort of re-summation is essential, and we do not yet know how to do it reliably. Even though each term of the perturbative expansion is singular at  $N = 0$ , it is rather sure that  $\mathbf{P}(N, \alpha_S)$  itself is not. Compare, for example, the expansion of

$$\sqrt{N^2 + \alpha_S} - N = \alpha_S/N + O(\alpha_S^2) \quad (12)$$

which is not valid if  $N < \alpha_S$ .



(a)



(b)

Fig. 10.  $\gamma p \rightarrow J/\psi p$ : data[18] for (a) the total cross section and (b) the differential cross section.

My own guess is that  $\mathbf{P}(N, \alpha_S)$  has no relevant singularity at all in the complex  $N$ -plane. If this is true, then the DGLAP evolution equation

$$Q^2 \frac{\partial \mathbf{u}(N, Q^2)}{\partial Q^2} = \mathbf{P}(N, \alpha_S) \mathbf{u}(N, Q^2) \quad (13)$$

is consistent with the approximation that  $\mathbf{u}(N, Q^2)$  just has poles, which are at fixed values of  $N$ , so yielding fixed powers  $f(Q^2)x^{-\epsilon}$  in  $F_2(x, Q^2)$  as in the fit (7). The evolution equation then tells us how  $f(Q^2)$  varies with  $Q^2$  at large  $Q^2$ .

In the ranges of  $x$  and  $Q^2$  where there are data for  $F_2(x, Q^2)$ , a conventional fit based on unresummed two-loop evolution and the two-pomeron fit can be made to agree well. But they do not continue to agree when we extrapolate them to smaller values of  $x$ , particularly at relatively small values of  $Q^2$ . This is seen in figure 11, which compares the two-pomeron fit (solid lines) with a two-loop-evolution fit[19].

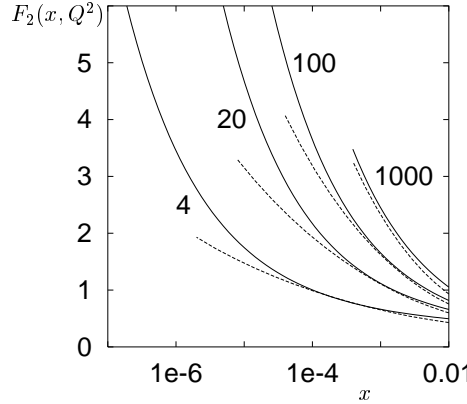


Fig. 11. Two-pomeron fit (upper curves) and two-loop-evolution fit (lower curves)

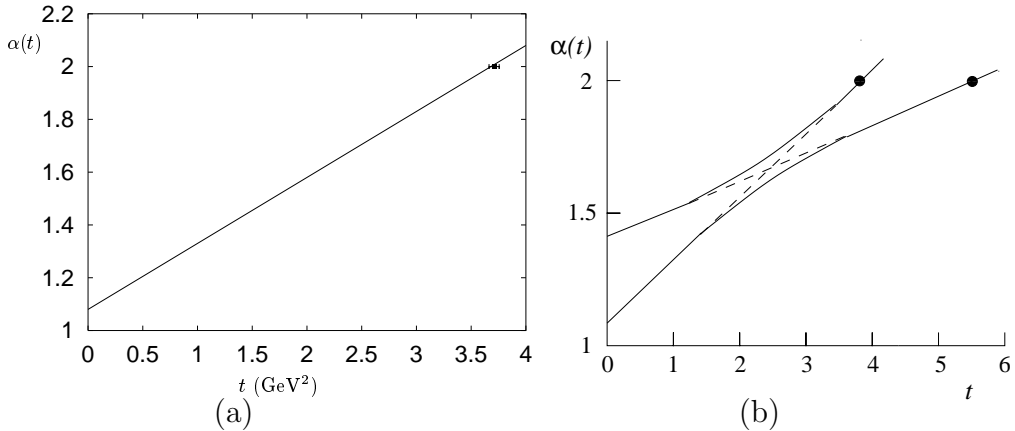


Fig. 12. Glueball trajectories: (a)  $2^{++}$  glueball candidate[20], with the trajectory (1); (b) repelling trajectories (1) and (5), with a second glueball candidate[21]

If indeed the hard and soft pomerons correspond to poles in the  $N$ -plane, they also correspond to poles in the complex angular momentum plane. In this case, for the value of  $t$  at which either trajectory passes through 2 there should be a particle with mass  $\sqrt{t}$ . Theoretical prejudice has it that these particles should be glueballs. Figure 12a shows that there is[20] a  $2^{++}$  glueball candidate with exactly the right mass to be on the soft-pomeron trajectory (1). There is a second such candidate[21] with the right mass to be on the hard-pomeron trajectory (5), but if two trajectories cross it is likely that they mix so that they avoid each other in the way shown in figure 12b. This picture gives the hard-pomeron trajectory a slope close to 0.1 as in (6).

## 6 Key questions

Among the key questions that I have raised in this talk are:

- Is a hard pomeron already present at  $Q^2 = 0$ ?
- Are there glueballs on pomeron trajectories?

- Will the hard pomeron be evident in  $pp$  total cross section at the LHC?
- Can we construct the theory of perturbative evolution at small  $x$ ?

## References

- [1] A Donnachie and P. V Landshoff, Physics Letters B296 (1992) 227
- [2] F Abe *et al*, CDF Collaboration, Physical Review D50 (1994) 5550
- [3] J. R Cudell *et al*, Physical Review D61 (1998) 034019
- [4] Particle Data Group, European Physical Journal C15 (2000) 1
- [5] G. A Jaroskiewicz and P. V Landshoff, Physical Review D10 (1974) 170
- [6] E Nagy *et al*, Nuclear Physics B150 (1979) 221
- [7] N. A Amos *et al*, E710 Collaboration, Physics Letters B247 (1990) 127
- [8] D Aston *et al*, Nuclear Physics B209 (1982) 56
- [9] J Breitweg *et al*, ZEUS Collaboration, European Journal of Physics C1 (1998) 81
- [10] A Donnachie and P. V Landshoff, Physics Letters B437 (1998) 408
- [11] A Donnachie and P. V Landshoff, hep-ph/0105088 (2001)
- [12] J Breitweg *et al*, ZEUS Collaboration, Physics Letters B487 (2000) 53
- [13] C Adloff *et al*, H1 Collaboration, European Physical Journal C19 (2001) 269
- [14] C Adloff *et al*, H1 Collaboration, European Physical Journal C21 (2001) 33
- [15] J Breitweg *et al*, ZEUS Collaboration, European Physical Journal C12 (2000) 35
- [16] G Abbiendi *et al*, OPAL Collaboration, European Physical Journal C14 (2000) 199
- [17] M Acciari *et al*, hep-ex/0102025 (2001)
- [18] C Adloff *et al*, H1 Collaboration, Physics Letters B483 (2000) 23
- [19] G Altarelli, R. D Ball and S Forte, Nuclear Physics B599 (2001) 383
- [20] S Abatzis *et al*, WA91 Collaboration, Physics Letters B324 (1994) 509
- [21] D Barberis *et al*, WA102 Collaboration, Physics Letters B397 (1997) 339